01 Aug 2015

Seismic-Hazard Map of Southeast Missouri and Likely Magnitude of the February 1812 New Madrid Earthquake

Jaewon Chung

J. David Rogers
Missouri University of Science and Technology, rogersda@mst.edu

Recommended Citation

J. Chung and J. D. Rogers, "Seismic-Hazard Map of Southeast Missouri and Likely Magnitude of the February 1812 New Madrid Earthquake," *Bulletin of the Seismological Society of America*, vol. 105, no. 4, pp. 2219-2234, Seismological Society of America, Aug 2015.
The definitive version is available at https://doi.org/10.1785/0120140307

Bulletin of the Seismological Society of America, Vol. 105, No. 4, pp. 2219–2234, August 2015, doi: 10.1785/0120140307

Seismic-Hazard Map of Southeast Missouri and Likely Magnitude of the February 1812 New Madrid Earthquake

by Jae-won Chung and J. David Rogers

Abstract The New Madrid seismic zone lies beneath the upper Mississippi Embayment, straddling the border between southeastern Missouri and northwestern Tennessee. In late 1811 and early 1812, it produced five earthquakes of magnitudes >6.5, violently shaking the central and eastern United States (CEUS). Its magnitude and recurrence are of concern to today's central United States regions. By considering the effects of local geology, deterministic scenario maps (M_w 7.3 and 7.7) were produced for ground motions intended to simulate the 7 February 1812 event (NM3), which was the largest felt. These maps include spatial estimates of peak ground acceleration and of 0.2 s and 1.0 s spectral acceleration (SA). Compared with the isoseismic map of modified Mercalli intensities (MMIs) in southeast Missouri, the MMIs converted from 0.2 s SA suggest that M_w 7.7 is a plausible scenario for NM3. To better constrain its magnitude, other CEUS sites shaken during NM3 were also examined. Local site conditions were studied and evaluated before calculating the threshold magnitude for the reported MMIs. These results indicate that the magnitude of NM3 was at least M_w 7.6, which validates our estimated size of M_w 7.7 for southeastern Missouri.

Introduction

With increasing frequency within the United States, seismically induced ground-shaking hazards are being spatially portrayed on geographic maps using geographic information systems (GIS). The information on these maps is most often conveyed in terms of peak ground acceleration (PGA) and spectral acceleration (SA). These can be used to estimate the severity of seismic site response to aid planners, engineers, and building officials in making decisions. PGA and SA values are also the important factors for assessing liquefaction potential and likely damage to man-made structures, respectively. These maps have been generated from either probabilistic seismic-hazard analyses (PSHA) or deterministic seismic-hazard analyses (DSHA; Krinitzsky, 2002; Cramer *et al.*, 2006). A PSHA map shows the spatial probability of exceeding a certain level of ground motion with all possible rupture scenarios but using different weightings. A DSHA map is used to assess ground motions for a specific magnitude and location of a historic or future earthquake as a scenario event (Cramer *et al.*, 2006; Frankel, 2013).

Effect of Site Conditions on Seismic Hazards

The peak ground motion and the response spectra are affected by local site/geologic conditions, including stiffness and thickness of unconsolidated sediments overlying bedrock (Seed *et al.*, 1976). Local site conditions are spatially variable and can thus amplify or deamplify seismic energy when the seismic waves propagate up through the soil cover, or cap. Historic earthquakes have demonstrated that local geologic conditions can significantly increase seismic damage. For instance, the M_s 8.1 Michoacán earthquake in 1985 struck Mexico City, more than 300 km from the epicenter, causing severe damage to a portion of the city. The affected area was a zone underlain by soft lacustrine deposits 30–45 m thick, which magnified the incoming seismic wavetrains because of the impedance contrast with long-period motions ($t > 1.0$ s). These soft soils amplified rock motions between 400% and 740% (Seed *et al.*, 1988). Virtually all of the high-rise buildings (7–22 stories high) collapsed or were severely damaged (Seed and Sun, 1987).

The U.S. Geological Survey (USGS) has produced and updated national PSHA maps, which present the expected rock motions from likely earthquakes emanating from known seismic zones in the western United States and central and eastern United States (CEUS; Frankel *et al.*, 2002; Petersen *et al.*, 2008, 2014). Their PSHA maps are constructed by assuming firm rock as the reference site condition with V_{S30} of 760 m/s (V_{S30} = average shear-wave velocity in the upper 30 m). This value is equivalent to the B/C site classification adopted by National Earthquake Hazard Reduction Program (NEHRP) in 2003 (Building Seismic Safety Council [BSSC], 2003).

Because the national PSHA maps do not consider the effects of actual geologic site conditions, these maps may

under- or overestimate the level or severity of shaking. To prepare realistic PSHA maps incorporating actual site effects, the variations in local site conditions (such as thickness of the soil cap) should be considered. Local site conditions are often a major factor in preparing realistic DSHA maps for scenario earthquakes. The DSHA maps can be treated as separate information and are useful in estimating ground motions during historical earthquakes bereft of seismic recordings. This is because the felt ground motions can be reproduced from the specific or repeat earthquakes in terms of their magnitude and/or assumed source zone (Krinitzsky, 2002; Haase and Nowack, 2011).

New Madrid Earthquakes

In the CEUS, the New Madrid seismic zone (NMSZ) in southeast Missouri has exhibited the highest seismicity, averaging about 200+ earthquakes greater than M 1.0 per annum (Missouri Department of Natural Resources Division of Geology and Land Survey [MODGLS], 2014). Since 1700, about 6259 earthquakes of $M \geq 2.5$ are reported to have occurred (Petersen *et al.*, 2014). Five earthquakes equal to M 3.0 are expected to occur each year (Boyd, 2010). The 1811–1812 earthquake sequences believed to have emanated from the NMSZ are the largest historic events (Williams *et al.*, 2010). The five mainshocks occurred on 16 December 1811 (three shocks; Fuller, 1912; Hough and Martin, 2002) noted as NM1 (Johnston, 1996), 23 January 1812 (NM2), and 7 February 1812 (NM3).

A repeat of this sequence would cause significant damage to the present-day central United States, which is criss-crossed by numerous pipelines, electric transmission lines, highways, and railroads that would be at considerable risk. Although the accurate evaluation of the 1811–1812 events is a critical factor to assess the seismic hazard in the areas adjacent to the NMSZ, the actual magnitudes are uncertain because no instruments recorded the earthquakes. These events are estimated to range between M 7.0 and 8.1, mainly based on felt reports.

The earthquake of 7 February 1812 (NM3) was the most severe of the 1811–1812 events, but its magnitude has been subject to considerable debate. Mueller and Pujol (2001) suggested NM3 ranges of M_w 7.2–7.4, based on the Reelfoot fault displacement of 1.5–3.1 m. With the assumption that the ruptures of the Reelfoot fault are 47.5–84.5 km long during NM3, Van Arsdale *et al.* (2013) estimated M_w 7.0–7.2, using published relationships between magnitude and fault rupture.

Johnston (1996) and Johnston and Schweig (1996) developed a regression of moment magnitude based on the macro-isoseismal area of intensities, suggesting a magnitude of M_w 8.0 for this event. Hough *et al.* (2000) lowered earlier felt intensities (modified Mercalli intensities [MMI]) by considering damage reports for structures at that time and site-response effects in the river valleys. They concluded its moment magnitude (M_w) to be between 7.4 and 7.5, applying the Johnston (1996) regression. Bakun and Hopper (2004) suggested M_w 7.8, based on the attenuation relationship between the MMI and distance (for eastern North America). They calculated site corrections with MMI and each likely magnitude. Later, Hough and Page (2011) reinterpreted MMIs with multiple experts' opinions and rescaled its magnitude to M_w 7.3 using Bakun and Hopper's method. Cramer and Boyd (2014) estimated it to be M_w 7.7 ± 0.3 (95% confidence level), based on mean MMI comparisons at large distances (600–1200 km) with known magnitudes.

These uncertainties with respect to the historical earthquakes results from different frameworks, including assigned MMIs, attenuation relations, and methods of computing magnitude. We noted that the effect of various site responses on estimating magnitude based on MMIs has historically been ignored or oversimplified (e.g., uniform thickness of alluvium over infinitely large areas) by previous studies (Hough *et al.*, 2000; Kochkin and Crandell, 2004; Street *et al.*, 2004). Historic records suggest that most settlements of the early 1800s were situated along the major watercourses on lowland alluvium, where seismic site response would significantly elevate MMIs. However, it is not true of all sites. For example, the site conditions in the urbanized boroughs of present-day St. Louis, Missouri, are not on Holocene alluvium, but on much stiffer residual soils blanketing the uplands (Street *et al.*, 2004). Street *et al.* (2004) pointed out that the magnitude of the 1811–1812 events would be underestimated by overestimating the site responses. In an attempt to understand the likely severity of the 1811–1812 events, site response should be estimated by properly accounting for local variances in depth, stiffness, and shear-wave velocities of the unconsolidated materials mantling each site.

In this study, we have attempted to account for site effects caused by variations of local geology in southeast Missouri, astride the NMSZ. Assuming the repeat of NM3, we prepared DSHA maps of PGA and SA at 0.2 and 1.0 s for M_w 7.3 and M_w 7.7 scenario earthquakes. We focused on NM3 for two reasons: it was the largest earthquake, and its rupture along the Reelfoot thrust was well documented at the time by eyewitnesses (Johnston and Schweig, 1996; Hough *et al.*, 2000; Hough and Page, 2011). We then constrained the plausible magnitude of NM3 by comparing the estimated ground motions with the felt reports. To better constrain the magnitude, we made a detailed compilation of subsurface site conditions at 25 CEUS sites that were shaken during NM3, then computed the threshold magnitudes to produce their reported MMIs.

Study Area

The study area encompasses 15 counties in southeastern Missouri in the upper Mississippi Embayment, west of the Mississippi River. The elevation of the area ranges from 70 to 540 m (Fig. 1). The underlying Paleozoic rock is principally composed of limestone and dolomite (Collinson *et al.*, 1988). The depths to the Paleozoic bedrock range from 6 to

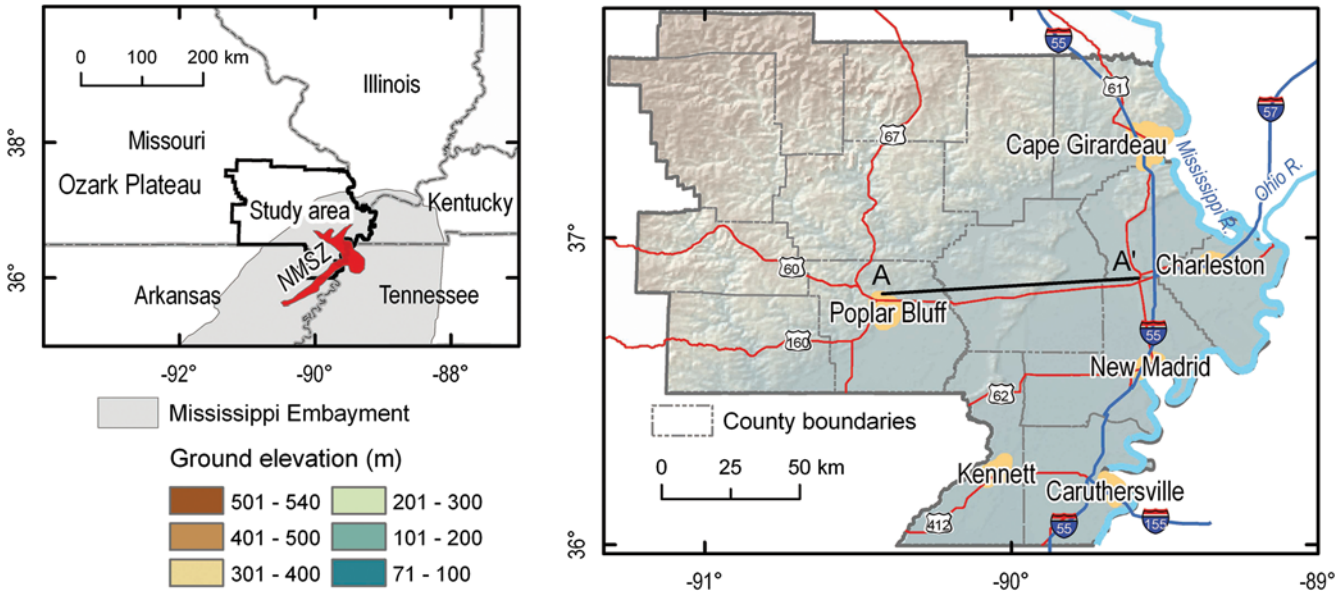

Figure 1. Location of study area, comprising 15 counties in southeastern Missouri, in the northern Mississippi Embayment and astride the New Madrid seismic zone (NMSZ). A–A′ shows the cross section in Figure 2. The color version of this figure is available only in the electronic edition.

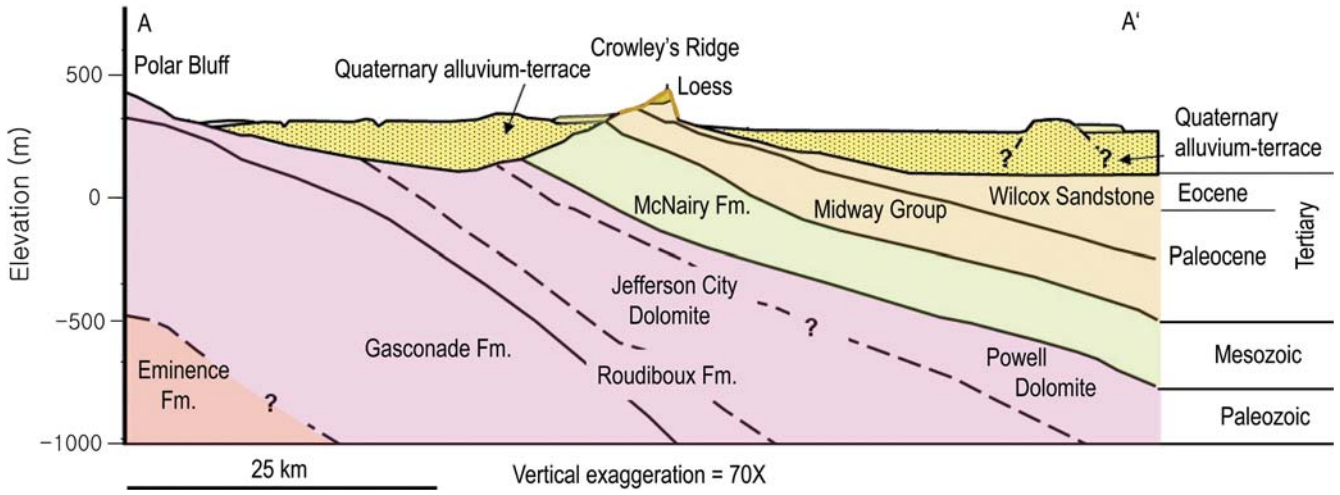

Figure 2. Generalized geologic cross section of the upper Mississippi Embayment (modified from Santi *et al.*, 2002). Location of the cross section is shown on the right side of Figure 1. Detailed explanation of geologic units is shown in Table A1. The color version of this figure is available only in the electronic edition.

600 m or deeper (Toro and Silva, 2001). The upper Tertiary strata are Claiborne (Eocene), Wilcox (Eocene–Paleocene), and Midway (Paleocene) groups (Fig. 2; Van Arsdale *et al.*, 1995; Santi *et al.*, 2002). An explanation of geologic units is shown in Table A1.

This region is characterized by two geomorphic provinces. The dissected uplands of the Ozark plateau form the bluffs extending from Cape Girardeau to Poplar Bluff. The southern area lies within the lowlands of the Mississippi Embayment (Fig. 1). The lowlands are composed of Quaternary alluvium deposited by the Mississippi and Ohio Rivers. Crowley's Ridge forms a long, narrow upland within the alluvial plain of the embayment. The ridge has been uplifted by Quaternary faulting and shaped by erosion of the Mississippi River (Van Arsdale *et al.*, 1995). Its surficial materials are composed of colluvium, capped by a thin loessal layer (Whitfield, 1982; Whitfield *et al.*, 1993). The Ozark uplands contain residual soils with decreasing thicknesses of loess moving away from the embayment (Fig. 3).

The NMSZ is a right-lateral system that cuts across the upper end of the Mississippi Embayment and is believed to be a failed intraplate rift dating back to the Precambrian. Although some possibility exists that several of the 1811–1812 epicenters may have been located outside of the NMSZ (e.g., NM2 in White County, Illinois, according to Hough *et al.*, 2005), these events are widely believed to have

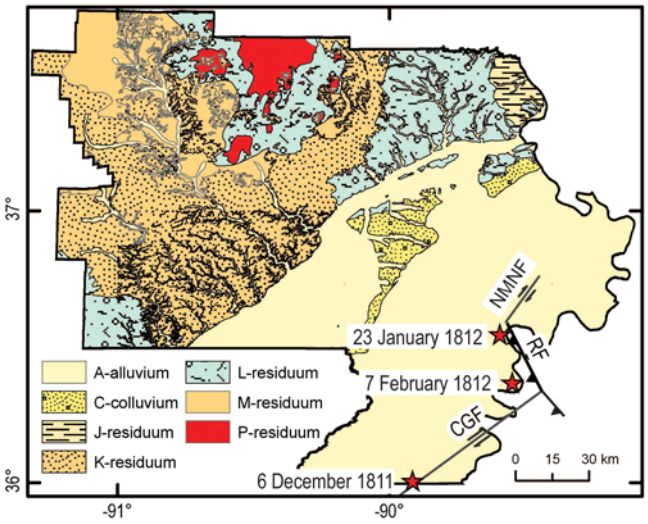

Figure 3. Simplified geologic map showing surficial materials (modified from Whitfield, 1982; Gray *et al.*, 1991; Whitfield *et al.*, 1993). Approximated epicenters of the largest 1811–1812 New Madrid earthquakes are shown with stars (modified from Williams *et al.*, 2010). Faults are delineated by solid lines (modified from Johnston and Schweig, 1996; Csontos and Van Arsdale, 2008). RF, Reelfoot thrust fault; CGF, Cottonwood Grove strike-slip fault (axial fault); and NMNF, New Madrid North fault. The color version of this figure is available only in the electronic edition.

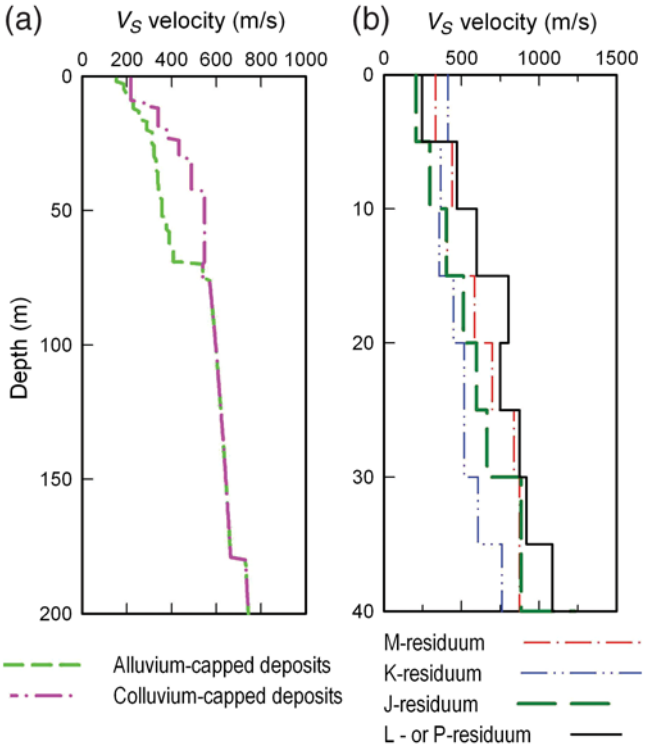

Figure 4. Reference shear-wave (V_S) velocity profiles for the surficial soils and unconsolidated sediments identified across the study area. (a) The profiles for alluvial and colluvial deposits in the Mississippi Embayment were modified from Romeo and Rix (2001. 2005) and Macpherson *et al.* (2010). (b) The profiles for residual soil deposits in the Ozark uplands were taken from *in situ* velocity measurements and/or standard penetration test blow counts. The color version of this figure is available only in the electronic edition.

occurred on the following fault systems: NM1 along the northeast-trending Cottonwood Grove strike-slip (right-lateral) segment of the NMSZ, NM2 along the New Madrid north fault, and NM3 along the northwest-trending Reelfoot thrust (Fig. 3; Johnston and Schweig, 1996; Odum *et al.*, 1998; Mueller *et al.*, 2004; Csontos and Van Arsdale, 2008; Van Arsdale *et al.*, 2013). Csontos and Van Arsdale (2008) interpreted that the Reelfoot fault is divided into a north fault (30° southwest dip) and a south fault (44° southwest dip) near the Cottonwood Grove fault. They also suggested that the Reelfoot south fault does not exhibit a surface scarp because its focal depths are deeper than those of the North fault. The 1811–1812 earthquakes caused severe shaking, with MMIs between VII and VIII (Hough *et al.*, 2000). The recurrence intervals of earthquakes large enough to trigger liquefaction are estimated to be somewhere between 500 and 750 years (Cramer, 2001; Tuttle *et al.*, 2002; Hough and Page, 2011; Frankel *et al.*, 2012).

The Wabash Valley seismic zone (WVSZ) lies along the border between Illinois and Indiana. It is believed to be capable of triggering an earthquake of M_w 6.5+ every 4000 years (Frankel *et al.*, 1996). In this study, we excluded the effects of the WVSZ in the seismic-hazard assessment of southeast Missouri, because we assumed that the NMSZ triggers the vast majority of significant earthquakes in the area of NM3. As more paleoseismic data is developed for the WVSZ, its relative contribution to the seismic hazard should be included in future assessments.

Data

This section describes the maps of reference profiles and bedrock depths (soil thickness) that influence site amplifications in the study area.

Reference Profiles

The dynamic properties of soils and rocks are considered controlling factors of site amplification, and their impact is usually estimated by considering the shear-wave (V_S) velocities of these materials (Gomberg *et al.*, 2003). A limited quantity of V_S data has been collected for the study area, so reference V_S profiles were established to generate characteristic models for the surficial geologic units (Fig. 4). For sediments in the Mississippi Embayment, the variations of V_S values with depth were estimated by equally weighting two previous studies of Romero and Rix (2001, 2005, weighted 0.5) and Macpherson *et al.* (2010, 0.5). These are shown in Figure 4a. For surficial soil cover in the Ozark uplands, we compiled data from 33 V_S *in situ* profiles and standard penetration test (SPT)-based V_S profiles. We used the conversion equation ($V_S = 85.34N^{0.348}$) proposed by

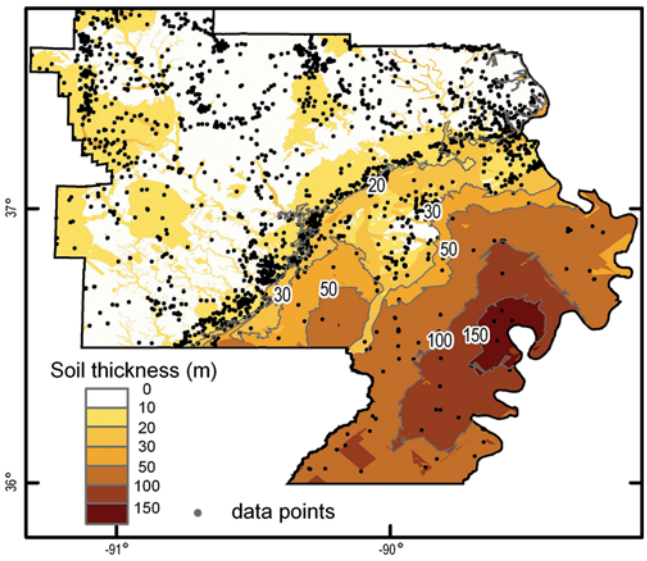

Figure 5. Interpolation of bedrock depths (soil thickness) in southeast Missouri using ordinary kriging. The color version of this figure is available only in the electronic edition.

Ohta and Goto (1978) to estimate V_S value from SPT blow counts (N). The reference profiles for the upland residual soils, loess, and colluvium are summarized in Figure 4b.

Soil Thickness

Where soil caps exhibit a narrow range of V_S velocities, the soil thickness (bedrock depth) usually emerges as the most important variable in estimating ground motion (Cramer, 2006; Haase *et al.*, 2010, 2011; Chung and Rogers, 2012a). The depth to bedrock overlying firm rock conditions (NEHRP site class B/C with V_S of 760 m/s) was estimated from borehole data culled from the subsurface database prepared by the Missouri Geological Survey (MODGLS, 2007). The database included 2639 boring logs across the project area (2038 in the uplands and 601 in the lowlands). The position of the bedrock surface was estimated as a depth beneath the existing ground surface rather than as an absolute bedrock elevation (Chung and Rogers, 2012b). To prevent over- or underestimation between different geomorphic provinces, we separately estimated bedrock depths for the uplands and the lowlands using ordinary kriging then compiled these data into a single map (Fig. 5).

The resultant map estimates that the depths to bedrock range from 0 to 20 m in the uplands and gradually increase toward the axis of the Mississippi Embayment, where it commonly exceeds 150 m. These values of the upper embayment are in good agreement with the V_S profiles with velocities of 760 m/s or greater, at depths between 100 and 160 m, which corresponds to the late Paleocene–early Eocene strata (Fig. 2; Santi *et al.*, 2002; Romero and Rix, 2005; Bailey, 2008; Macpherson *et al.*, 2010). Ordinary kriging provided geostatistical measures of uncertainty associated with the depth to bedrock estimates. In areas where fewer data points exist, the kriging map assigns the greatest uncertainty.

Scenario Earthquake Hazards

The DSHA map shows PGAs at the ground surface and SAs at 0.2 s (5 Hz) affecting one- and two-story structures (with short fundamental periods, T) and 1.0 s (1 Hz) for buildings (10+ stories high) with longer fundamental periods (T).

Approach

To evaluate deterministic hazards for earthquake scenarios, the impact of site effects on seismic ground motion were calculated at grid points spaced 1 km apart, across the study area. Each grid point was assigned by the corresponding input parameters, such as (1) the surficial geologic unit and its reference V_S soil profile with material properties (e.g., density and soil type with/at depth), (2) the thickness of the soil profile overlying the bedrock, and (3) the attenuated rock motion from an assumed source.

Scenario Earthquakes. Two events of M_w 7.3 and 7.7 were employed for scenario earthquakes. These scenarios are similar to those used in the models generated by the USGS for the CEUS (Petersen *et al.*, 2008). Petersen *et al.* (2008) applied lowest weight (0.15) for the M_w 7.3 event and the highest weight (0.5) for the M_w 7.7 event in developing the 2008 USGS maps. The scenario earthquakes assume ruptures along the Reelfoot thrust, as most believe to have occurred during NM3. This study employed a rupture length of 60 km and a width of 10 km for the M_w 7.3 scenario, and a width of 20 km for the M_w 7.7 event along the Reelfoot thrust, suggested by Cramer (2001).

Attenuation Relations. The attenuation relations were used to estimate the rock motion in seismic waves with increasing distance from the seismic source. With several attenuation relations previously developed for the CEUS, we employed the USGS weighting scheme (Petersen *et al.*, 2014): Toro *et al.* (1997; weighted 0.11), Silva *et al.* (2002; 0.06), Frankel *et al.* (1996; 0.06), Atkinson and Boore (2006; 0.22), Somerville *et al.* (2001; 0.1), Campbell (2003; 0.11), Tavakoli and Pezeshk (2005; 0.11), Atkinson (2008, 0.08), and Pezeshk *et al.* (2011, 0.15). Figure 6 shows the weighted averages of attenuation relations (hard rock) at PGA and 0.2 and 1.0 s SA as a function of distance for scenario earthquakes (M_w 7.3 and 7.7). The weighted attenuation relations were optimized for hard-rock sites (NEHRP site class A). We consider firm-rock sites (NEHRP site class B/C) as the reference points for estimating rock motions. To convert from hard-rock to firm-rock site conditions, we applied the modification factors suggested by Frankel *et al.* (1996): 1.52 for PGA, 1.76 for 0.2 s SA, and 1.72 for 1.0 s SA.

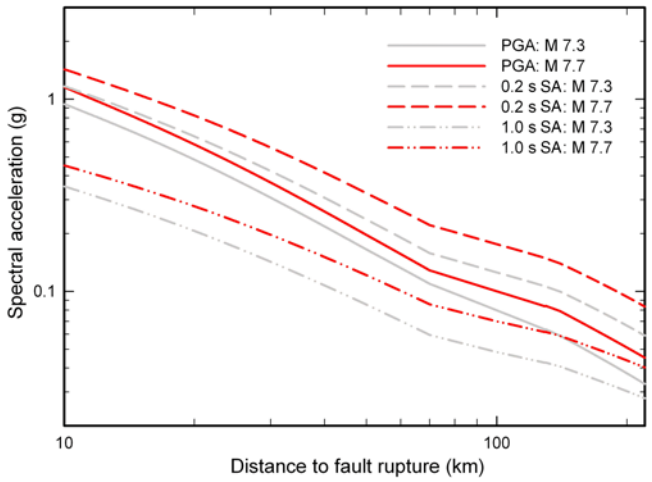

Figure 6. The hard-rock attenuation relations for peak ground acceleration (PGA) and 0.2 and 1.0 s spectral acceleration (SA) with distance for M_w 7.3 and 7.7 earthquakes. We adopted the U.S. Geological Survey weighted scheme (Petersen *et al.*, 2014) for central and eastern United States (CEUS) hard-rock attenuation. The color version of this figure is available only in the electronic edition.

Time Histories. The input time histories for M_w 7.3 and 7.7 events were simulated using Stochastic Method SIMulation (SMSIM) v.2.3 code (Boore, 2005), in the absence of recorded motions for large earthquakes ($M_w > 6.5$) in the CEUS (Atkinson and Beresnev, 2002; Ramírez-Guzmán *et al.*, 2012). The SMSIM time series are generated from the transformation of empirical acceleration spectra of historic earthquakes. Stochastic models assume that a fault at a point source may radiate randomly for a certain duration, which depends on the size and distance to the earthquake (Boore, 2003). The total point-source spectrum of rock motion was expressed as

$$\mathrm{Acc}(M_0, R, f) = CS(M_0, f)D(R, f)I(f),$$

in which $\mathrm{Acc}(f)$ is the total point-source spectrum of acceleration at bedrock; C is a scaling factor; $S(f)$ is the source spectrum; $D(f)$ is the diminution function (geometrical spreading and inelastic attenuation) to modify the spectral shape; $I(f)$ is a filter to shape the spectrum; M_0 is seismic moment; R is the distance from the source; and f is the frequency.

Ten time histories were generated for input rock motions from 0.05 to 1.5g, which were estimated from attenuation relations.

Ground-Motion Estimates. The site-response analysis at each grid point was performed using DEEPSOIL software (Hashash *et al.*, 2012). DEEPSOIL is appropriate to evaluate site responses of thick sediments in the Mississippi Embayment with 1D nonlinear or equivalent linear analysis of a multilayer profile on a rigid half-space subjected to input rock motion (Cramer, 2006; Hashash *et al.*, 2012).

Compared to nonlinear analyses, equivalent linear analyses require less computation, because they consider the isotropic soil stiffness and damping ratio of the soil layer. Equivalent linear approaches approximate acceptable ground motions for rock motions less than 0.2g and produce similar results with nonlinear approaches, for rock motions subjected to between 0.05 and 0.50g (Idriss, 1990; Electric Power Research Institute, EPRI, 1993). The rock motion of the study area lies mainly within 0.50g, except areas <30 km from fault rupture. We chose to use the equivalent linear approach because it requires simple process and produces reasonable results for the study area (Kramer, 1996; Hashash *et al.*, 2010).

Assuming soil stiffness and damping are most influenced by shear strain, we employed an equivalent linear approach in the frequency domain with a 5% damping ratio. After calculations were made for various combinations of reference V_S profiles, bedrock depths, and rock motions, SAs at PGA, 0.2 s, and 1.0 s were assigned to each grid point with corresponding input parameters and amplification factors. The values for the intervening areas between the 1 km grid points were then interpolated using ordinary kriging to produce the DSHA map incorporating the local geologic conditions.

Seismic-Hazard Maps

The resultant maps (Fig. 7) of PGA, 0.2 s, and 1.0 s SA suggests that the upper Mississippi Embayment exhibits a range of SAs: PGA with 0.18–1.5g and 0.2–2.0g, 0.2 s SA with 0.35–2.3g and 0.5–2.7g, and 1.0 s SA with 0.16–1.3g and 0.2–1.7g for M_w 7.3 and 7.7 earthquakes, respectively. The Ozark uplands exhibited PGA with 0.05–0.15g and 0.07–0.2g, 0.2 s SA with 0.1–0.25g and 0.12–0.5g, and 1.0 s SA with 0.05–0.15g and 0.06–0.17g for M_w 7.3 and 7.7 earthquakes, respectively.

MMI Maps. We also attempted to estimate MMI values based on ground motions produced in this study. The recorded or simulated ground-motion parameters have been correlated to estimate MMI values. Recent studies (Kaka and Atkinson, 2004; Atkinson and Kaka, 2007; Dangkua and Cramer, 2011) developed predictive correlations for the CEUS. For quantitative estimates of MMIs, the values of PGA and 0.2 s SA were converted into MMI values (Figs. 8 and 9, respectively). For this procedure, we employed the empirical relationships between MMI and PGA (Atkinson and Kaka, 2007; Dangkua and Cramer, 2011) and between MMI and 0.2 s SA (Kaka and Atkinson, 2004; Table 1). The MMI contours for M_w 7.3 and 7.7 earthquakes were compared with those delineated by Hough *et al.* (2000). The comparisons are shown for PGA-based MMIs (Fig. 8) and for 0.2 s SA-based MMIs (Fig. 9). The PGA-based MMIs are between IV and VI in the Ozark uplands and between VII and X in the upper Mississippi Embayment for the M_w 7.3 (Fig. 8a) event; they are between V and VI in the uplands and between VII and X in the upper embayment for the M_w 7.7 earthquake (Fig. 8b).

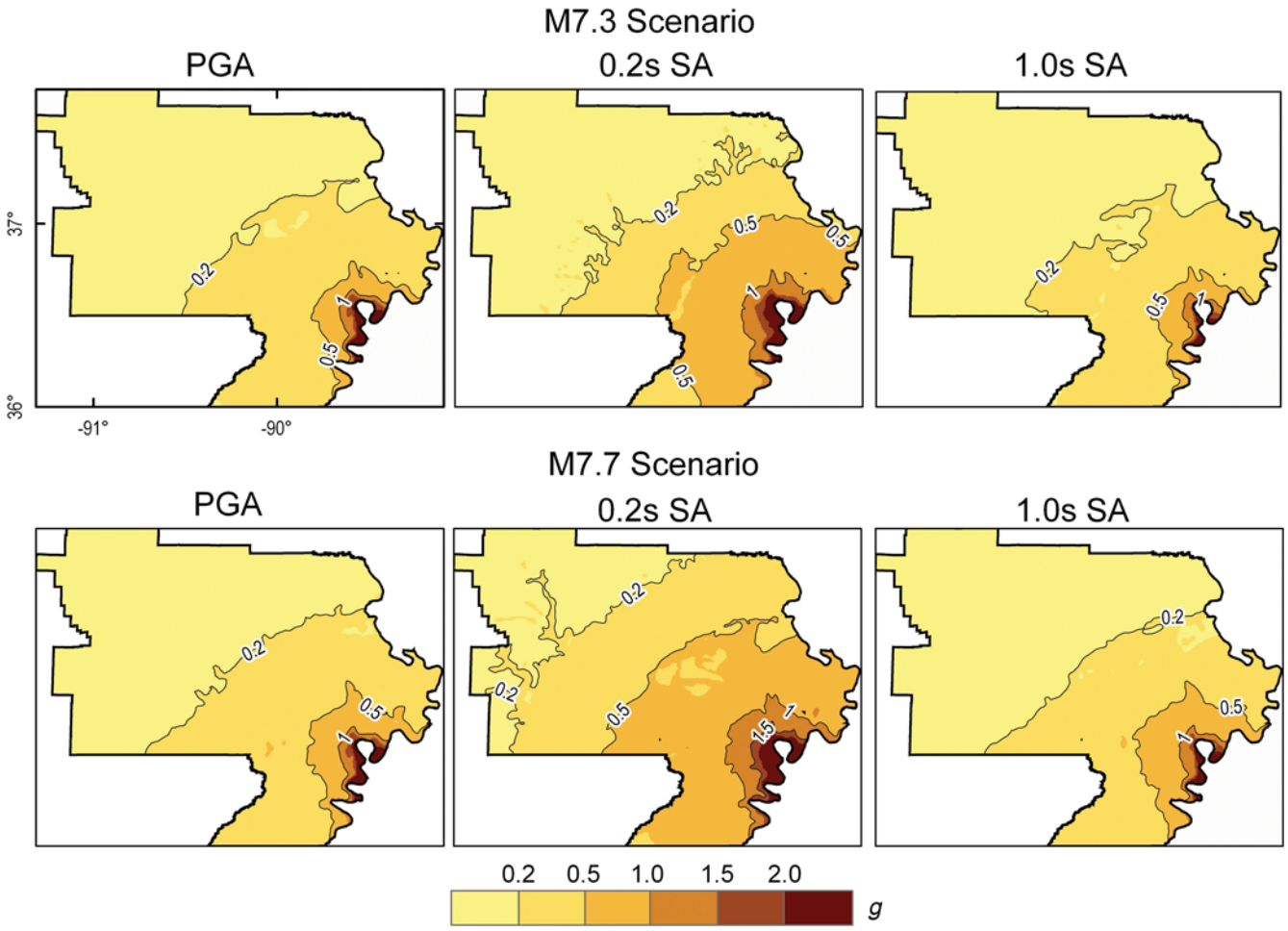

Figure 7. Deterministic seismic-hazard analysis maps for M_w 7.3 and 7.7 scenario earthquakes on the Reelfoot thrust with strike-slip faults in the NMSZ, corresponding to the likely range of seismicity experienced in the 7 February 1812 New Madrid earthquake (NM3). The color version of this figure is available only in the electronic edition.

Magnitude Estimation from MMI Contours. Hough *et al.* (2000) generated an isoseismal map based on reported damage to houses, including distressed chimneys, during NM3 (the only settlements in that area along the Mississippi River at the time were New Madrid, Caruthersville, and Cape Girardeau). The 0.2 s SA was selected among the ground-motion parameters for comparison because it approximates the fundamental period (T) of a two-story building. We then matched our 0.2 s SA-based MMIs with the observation-based MMIs, which is considered to be a close approximation.

The resultant map for an M_w 7.3 event shows MMIs of VI–VII in the uplands and VII–IX in the embayment (Fig. 9a), and the map of an M_w 7.7 earthquake suggests that the predominant MMIs are VII in the uplands and VIII–X in the embayment (Fig. 9b). This suggests that the MMI estimates for an M_w 7.7 event provide the best match with the observations reported in 1812 (mostly VII for the uplands and VIII for the embayment). We estimate that the magnitude of the NM3 event was likely closer to 7.7 to generate ground motions with extensive MMIs of VII and VIII in the uplands and the embayment, respectively. This is consistent with the previous interpretations of Atkinson and Beresnev (2002). They noted that magnitudes of the 1811–1812 earthquakes likely ranged between 7.5 and 8.0, based on their simulated ground motions and subsurface data in the St. Louis and Memphis metro areas.

Magnitude Estimates from Other CEUS Sites

To better quantify and constrain the likely magnitude of NM3, we examined the local site conditions of 25 damaged CEUS sites across the upper Embayment. We then attempted to estimate the threshold magnitudes corresponding to the reported MMIs, using the regression analysis for the CEUS. This procedure included the following steps:

1. calculate the median values of interpreted MMIs for each site during NM3,
2. examine soil amplification from V_{S30} values,
3. calculate 0.2 s SA and peak ground velocity (PGV) with changing magnitudes,
4. convert these values into MMI values,

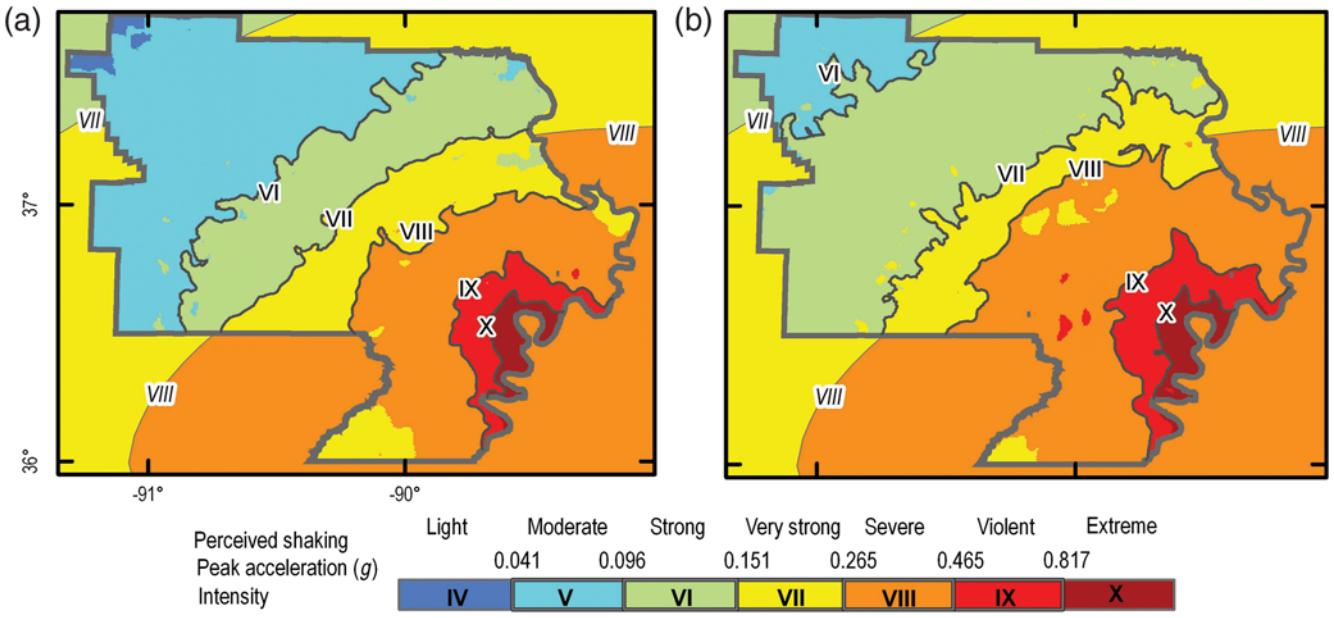

Figure 8. Modified Mercalli intensity (MMI) maps for (a) the M_w 7.3 earthquake and (b) the M_w 7.7 earthquake on the Reelfoot thrust. MMI contours were inferred from PGA calculated in this study (Fig. 7), based on MMI–PGA relationships (Atkinson and Kaka, 2007; Dangkua and Cramer, 2011). The MMI contours of Hough *et al.* (2000) were used as a background for comparison. The solid line delineates the study area, and the area bounding this is taken from Hough *et al.* (2000). Note that Hough *et al.* did not contour MMIs of IX–X in the embayment. The color version of this figure is available only in the electronic edition.

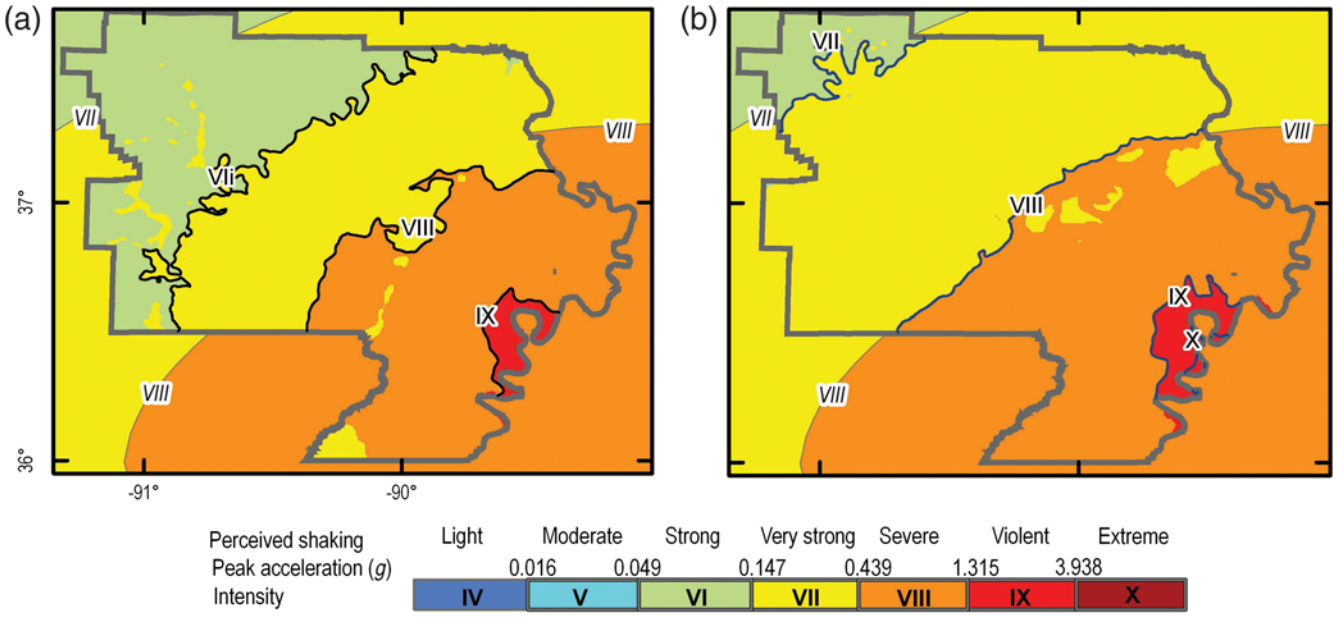

Figure 9. MMI maps for (a) the M_w 7. 3 earthquake and (b) the M_w 7.7 earthquake. In this case, MMIs were inferred from 0.2 s SA (Fig. 7) based on MMI–0.2 s SA relationships (Kaka and Atkinson, 2004). The MMI contours of Hough *et al.* (2000) were used as a background for comparison. The color version of this figure is available only in the electronic edition.

5. estimate the threshold magnitudes for corresponding MMIs,
6. constrain the likely magnitude for NM3.

We used the MMIs to estimate the magnitude of NM3, assuming that the reported MMI values were reliable estimates of shaking intensity to calculate the magnitude of the historical earthquake (Johnston, 1996; Hough *et al.*, 2000) based on the relationship between magnitude and MMIs as a function of distance. However, the magnitude uncertainty of the 1811–1812 earthquakes is tied to the MMI

Table 1
Peak Ground Velocity (PGV), Peak Ground Acceleration (PGA), and 0.2 s Spectral Acceleration (SA) Ranges for Modified Mercalli Intensities (MMIs)

MMI	PGV (cm/s)*	PGA (g)*	0.2 s SA (g)†
IV	0.6–2.9	0.008–0.041	0.005–0.016
V	2.9–5.2	0.041–0.067	0.016–0.028
V–VI	5.2–6.5	0.067–0.096	0.028–0.049
VI	6.5–9.5	0.096–0.114	0.049–0.085
VI–VII	9.5–13.8	0.114–0.151	0.085–0.147
VII	13.8–20.3	0.151–0.200	0.147–0.254
VII–VIII	20.3–29.6	0.200–0.265	0.254–0.439
VIII	29.6–63.4	0.265–0.465	0.439–1.315
IX	63.4–135.5	0.465–0.817	1.315–3.938
X	> 135.5	> 0.817	> 3.938

*Modified from Atkinson and Kaka (2007) and Dangkua and Cramer (2011).
†Modified from Kaka and Atkinson (2004).

uncertainty, because many of the MMI values are inconsistent with the reported distances to adequately constrain the magnitude. Of MMI uncertainty, we point out that the different site responses would have produced considerable variability in reported MMI values, even at similar distances from the earthquake source. Previous research (Hough *et al.*, 2000; Bakun and Hopper, 2004; Hough and Page, 2011) noted that the site conditions of river valleys have increased the reported MMIs during the 1811–1812 events. The MMIs that are properly inferred by consideration of site effects thus would reduce the magnitude uncertainty of historical earthquakes.

MMIs during NM3

Historical MMIs for NM3 have been interpreted with felt reports accounting for structural damages to buildings (Hough *et al.*, 2000). Most structures constructed prior to 1811 in the central United States were one to two-and-a-half stories high (Kochkin and Crandell, 2004), which are sensitive to ~0.2 s SA. This suggests that the fundamental period of buildings damaged during NM3 is likely close to ~0.2 s. For this reason, 0.2 s SA would appear to be an appropriate ground-motion parameter for estimating MMIs during NM3. PGV is the preferred indicator of ground-motion parameters to estimate MMI as well, because it correlates well with the observed intensity for earthquakes (Wald *et al.*, 1999; Boatwright *et al.*, 2001; Kaka and Atkinson, 2004). The values of PGV were converted into MMI values based on the empirical relationships (Atkinson and Kaka, 2007; Dangkua and Cramer, 2011; Table 1).

Macroseismic data of MMIs for NM3 have been revised according to the damage descriptions. Interpreted MMIs at 25 sites were compiled from previous studies (Hough *et al.*, 2000; Bakun *et al.*, 2002; Hough and Page, 2011). We selected sites with MMIs ≥V for better constraint; magnitude tends to be overestimated by MMIs lower than V, and it is hard to differentiate low intensities based on the felt and damage reports (Bakun and Wentworth, 1997; Wald *et al.*, 1999; Kaka and Atkinson, 2004). A set of MMIs at each site consists of six values, including one from Hough *et al.* (2000), one from Bakun *et al.* (2002), and four from Hough and Page (2011). The median was then calculated from six MMI values. Locations of the 25 sites are shown in Figure 10, and the MMIs and their respective distances from the fault rupture of NM3 are listed in Table 2.

Estimation of Magnitude

Based on magnitude, distance to fault, and site effects, the 0.2 s SAs and PGV values were analyzed using the Atkinson and Boore (2006) equations (see the Appendix). These equations were developed to simulate ground motions for hard rock and soil sites, based on CEUS seismographic data and the extended finite-fault simulation (EXSIM) code. Their equations provide good approximations of seismic ground motions for eastern North America (Atkinson and Boore, 2006).

Site Conditions. According to the equations of Atkinson and Boore (2006), the local site conditions influencing the site effects can be calculated from V_{S30} values. Previous investigators (Wald and Allen, 2007; Iwahashi *et al.*, 2010) validated the method for estimating V_{S30} values using digital elevation models (DEMs). This method assumes that topographic gradients correlate with V_{S30} values; for example, slope steepness is proportional to V_{S30}. We previously mapped V_{S30} values across the St. Louis metropolitan area using ~1500 V_{S30} datasets (Chung and Rogers, 2012a). The DEM-based site classifications for the St. Louis area (Allen and Wald, 2009) are very similar to our results, suggesting that DEMs can be used as a proxy for site conditions. From the V_{S30} map server and Quaternary geologic maps of USGS (see Data and Resources), we explored V_{S30} values and surficial materials for CEUS historic sites, by examining historic maps from the early 1800s. As shown in Table 2, V_{S30} values of each CEUS site vary locally. For instance, it was reported that the settlements comprising St. Louis in the early 1800s were along the banks of the Mississippi River (St. Louis City Plan Commission, 1969; Faherty, 1990). Our examination of these factors suggests that the site conditions (V_{S30}) range between 305 and 509 m/s (Fig. 11a).

Magnitude for MMI. Using the prediction equation shown in the Appendix, ground motions were also estimated as a function of magnitude then converted to MMI, based on the MMI–0.2 s SA and the MMI–PGV relationships (Table 1). For each site, the threshold magnitudes corresponding with MMIs for various V_{S30} site conditions were then estimated.

For instance, MMIs of VII were assigned for the St. Louis area during NM3 (Table 2). Using the regression equation in the Appendix, the calculated threshold magnitudes for MMI VII are M_w 7.7–9.0 for 0.2 s SA (Fig. 11b)

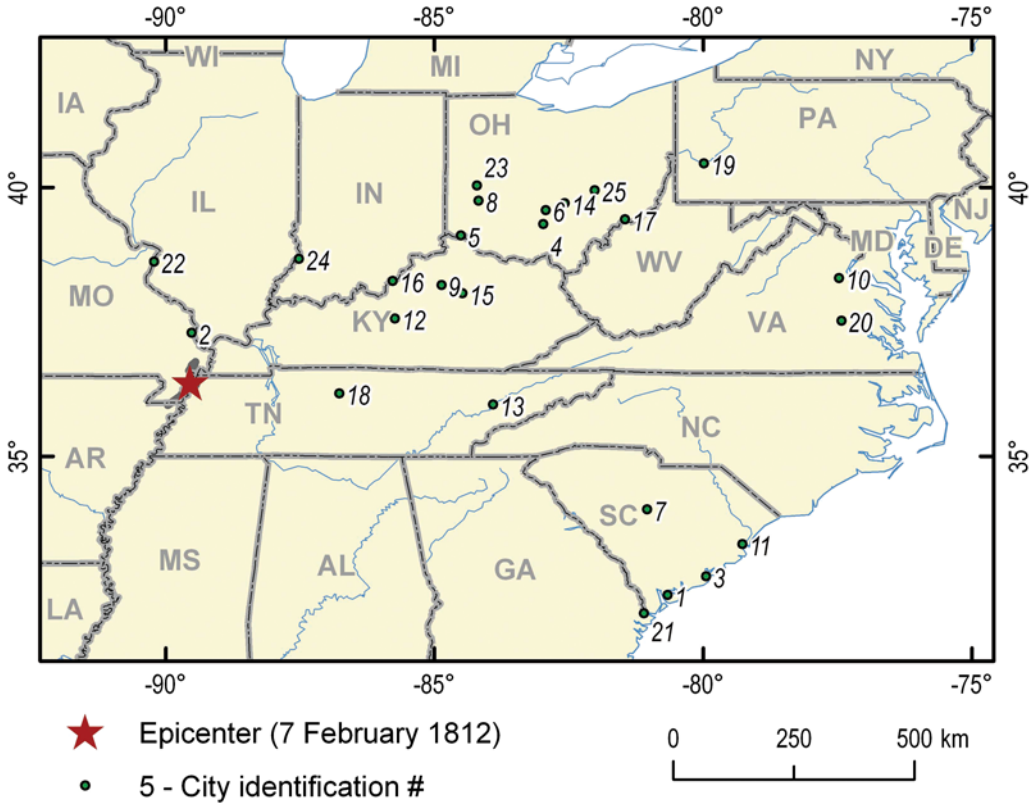

Figure 10. Location map showing the CEUS sites shaken during NM3. The MMI values for each site are listed in Table 2. The color version of this figure is available only in the electronic edition.

and M_w 7.8–8.6 for PGV (Fig. 11c). Similarly, the threshold magnitudes for other sites were calculated as a function of site conditions, distance from seismic source, and the assigned MMIs during NM3.

As shown in Table 2 and Figure 12, the threshold magnitudes for assigned MMIs at each site vary, depending on the respective site conditions. We attempted to constrain the magnitude of NM3 with the magnitude satisfying the most sites for 0.2 s SA and PGV. Of the 25 sites, M_w 7.6 was the threshold magnitude with the largest frequency in estimated values, with 13 sites for 0.2 s SA and 13 sites for PGV (Figs. 12 and 13). Both the median and the mean are M 7.7 for 0.2 s SA and M_w 7.7 for PGV. The mode, median, and the mean that are measures of central tendency fall within M_w 7.6–7.7 (Fig. 13), suggesting M_w 7.6 would be the representative value of threshold magnitude without the skewness in data distribution.

This suggests that the magnitude of NM3 would have been at least M_w 7.6, and this value agrees well with M_w 7.7, which was estimated from the simulated ground motions for southeast Missouri. Meanwhile, the median and the mean with standard deviation of threshold magnitude, not considering site effects (e.g., a single site condition as hard rock), are M_w 8.1 and M_w 8.1 $\pm$ 0.5, respectively (Table 2 and Fig. 12). This suggests that the threshold value bereft of considering site effects of the early 1800s communities would be overestimated for the likely magnitude of NM3, compared with those estimates considering site effects.

Discussion and Conclusions

This article presents earthquake hazard maps of ground motions in southeastern Missouri that consider site effects imposed by surficial geology on input rock motions, simulating the New Madrid earthquake on 7 February 1812 (NM3). These hazard maps can be used to aid decisions by building officials, urban planners, consultants, insurance carriers, utilities, emergency response agencies, and state and federal transportation authorities to better estimate the areal distribution of shaking severity and earthquake hazards. They are also useful in helping to assess paleoseismic aspects of ground shaking and for estimating the likely magnitudes of prehistoric and preinstrument earthquakes.

By considering reference V_S profiles for each geologic unit truncated by bedrock depths, DSHA maps were produced for M_w 7.3 and 7.7 scenarios, which are assumed to bracket the New Madrid earthquake of 7 February 1812 (event NM3).

By using a 1D site response program, such as SHAKE or DEEPSOIL (used in this study), the DSHA maps were constructed using scenario seismicity as their primary sources of input. This approach possesses inherent uncertain-

Table 2

Threshold Magnitude for Reported Modified Mercalli Intensities (MMIs) during the 7 February 1812 (NM3) Earthquake

Number	Location	State	MMI	Longitude (°)	Latitude (°)	Distance from Epicenter (km)	V_{S30} (m/s)	Surficial Material	Threshold Magnitude			
									With No Site Effect		With Site Effect	
									0.2 s SA	PGV	0.2 s SA	PGV
1	Beaufort	South Carolina	VI	−80.662	32.421	932	365–488	Paludal deposits	> 9.0	8.7	> 9.0	8.1–8.3
2	Cape Girardeau	Missouri	VII–VIII	−89.521	37.296	100	305–456	Alluvium or residuum	8.7	8.9	8.0–8.3	8.2–8.5
3	Charleston	South Carolina	V	−79.946	32.771	973	255–349	Paludal deposits	8.3	7.9	7.4–7.7	7.2–7.4
4	Chillicothe	Ohio	VI	−82.979	39.321	600	232–346	Till or alluvium	8.8	8.3	7.6–7.9	7.4–7.8
5	Cincinnati	Ohio	VI	−84.512	39.104	520	487–760	Till	8.2	8.2	7.8–8.2	7.9–8.2
6	Circleville	Ohio	VI	−82.929	39.579	665	180–357	Till	> 9.0	8.3	7.6–8.3	7.3–7.8
7	Columbia	South Carolina	VI	−81.046	34.013	823	319–760	Residuum	> 9.0	8.5	> 9.0	7.9–8.5
8	Dayton	Ohio	V–VI	−84.179	39.754	603	286–388	Till	7.5	7.9	7–7.2	7.3–7.5
9	Frankfort	Kentucky	VI	−84.871	38.188	440	446–760	Residuum	7.8	8.1	7.4–7.8	7.8–8.1
10	Fredericksburg	Virginia	V	−77.471	38.313	1070	338–570	Residuum	> 9.0	8.0	8.1–8.4	7.5–7.8
11	Georgetown	South Carolina	V	−79.271	33.371	1001	255–349	Paludal deposits	8.5	7.9	7.5–7.8	7.2–7.5
12	Hodgenville	Kentucky	V–VI	−85.738	37.563	350	311–531	Residuum	6.7	7.6	6.4–6.6	7.1–7.4
13	Knoxville	Tennessee	V	−83.912	35.963	500	266–760	Residuum	6.6	7.5	6.2–6.6	7.3–7.5
14	Lancaster	Ohio	V–VI	−82.579	39.704	715	264–466	Till	8.1	8.0	7.6–7.7	7.6–7.7
15	Lexington	Kentucky	VI	−84.479	38.029	486	329–597	Residuum	8.0	8.2	7.5–7.8	7.6–8.0
16	Louisville	Kentucky	VI–VII	−85.779	38.263	395	180–232	Alluvium	9.0	8.5	7.4–7.6	7.4–7.6
17	Marietta	Ohio	V–VI	−81.454	39.404	780	324–760	Colluvium	8.5	8.0	7.7–8.5	7.5–8.0
18	Nashville	Tennessee	VI–VII	−86.771	36.171	250	285–760	Alluvium	7.9	8.2	7.2–7.9	7.6–8.1
19	Pittsburgh	Pennsylvania	V	−79.988	40.446	930	413–602	Colluvium	8.1	7.8	7.6–7.9	7.5–7.7
20	Richmond	Virginia	V	−77.429	37.521	1070	338–587	Residuum	> 9.0	8.0	8.1–8.8	7.5–7.8
21	Savannah	Georgia	V	−81.104	32.079	920	218–513	Paludal deposits	8.0	7.8	7.1–7.7	7.0–7.6
22	St. Louis	Missouri	VII	−90.221	38.621	230	305–509	Till or alluvium	> 9.0	8.7	7.7–9.0	7.8–8.6
23	Troy	Ohio	V–VI	−84.213	40.037	600	206–358	Till or alluvium	7.5	7.9	6.8–7.1	7.0–7.4
24	Vincennes	Indiana	VI–VII	−87.521	38.671	313	232–760	Till	8.2	8.4	7.3–8.2	7.5–8.4
25	Zanesville	Ohio	V–VI	−82.021	39.946	750	206–760	Colluvium	8.3	8.0	7.2–8.3	7.6–8.0
								Mode	n.a	n.a	7.7	7.6
								Mean	8.0 ± 0.6	8.1 ± 0.3	7.7 ± 0.5	7.7 ± 0.3
								Median	8.1	8.0	7.7	7.7
								Mean for 0.2 s SA and PGV		8.1 ± 0.5		7.7 ± 0.4
								Median for 0.2 s SA and PGV		8.1		7.7

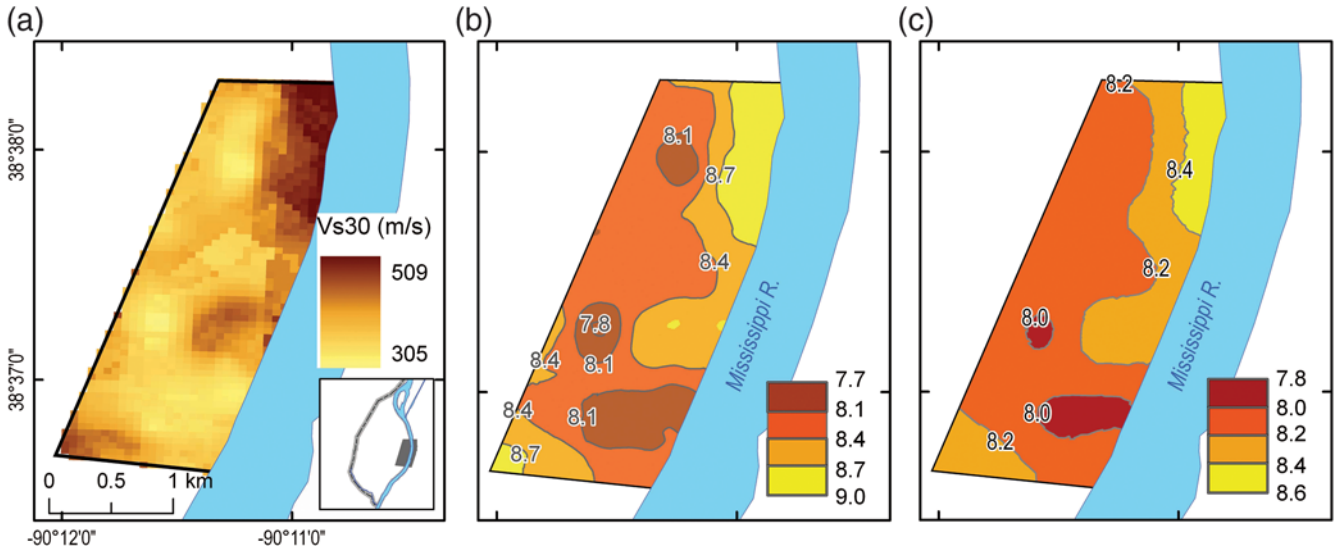

Figure 11. (a) V_{S30} values of early 1800s settlement sites in the St. Louis area, Missouri. (b) Spatial threshold magnitudes for 0.2 s SA to produce an MMI of VII. (c) Spatial threshold magnitudes for peak ground velocity (PGV) to produce an MMI of VII. The color version of this figure is available only in the electronic edition.

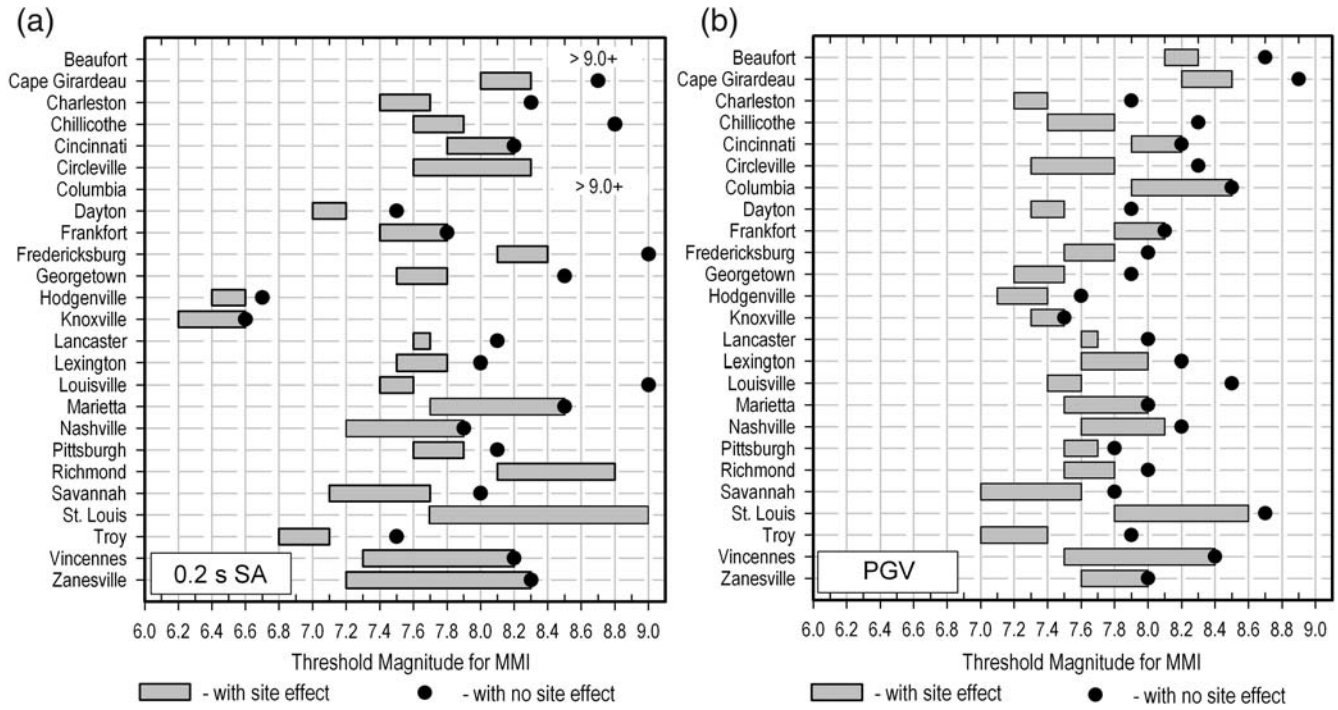

Figure 12. Ranges of calculated threshold magnitude for (a) 0.2 s SA and (b) PGV to produce the reported MMIs at CEUS sites during NM3. Threshold magnitude varies depending on local site amplification as a function of V_{S30} at a given MMI value.

ties in input parameters (Cramer, 2001; Chapman *et al.*, 2006; Cramer *et al.*, 2006), such as (1) input time histories, (2) attenuation relations, and (3) reference V_S soil profiles. Of these input parameters, the input time histories and the attenuation relations appear to be the most important parameters for site-response modeling (Newman *et al.*, 2001; Destegul, 2004; Karadeniz, 2008). A detailed sensitivity analysis was beyond the scope of this article.

As a result of the lack of time histories of M_w 6.0+ events emanating from the NMSZ, we simulated base rock earthquake records using the Boore (2005) code. More credible synthetic earthquake models need to be generated for the

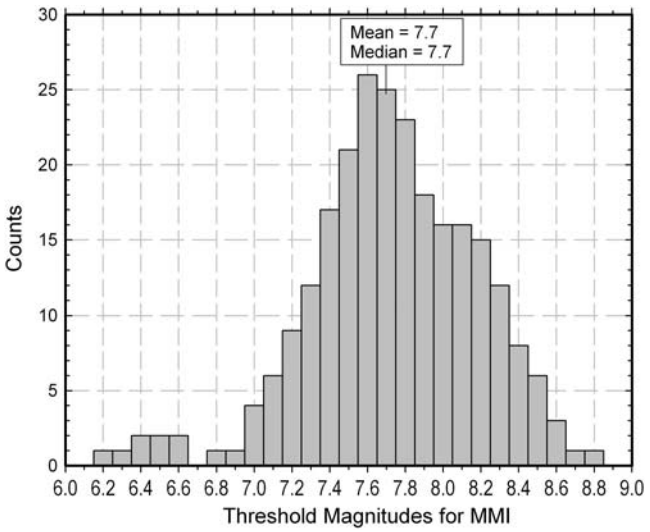

Figure 13. Histograms of threshold magnitudes for both 0.2 s SA and PGV shown in Figure 12. The mode is M_w 7.6. The median and the mean both are M_w 7.7.

CEUS, because the region exhibits much higher impedance contrasts than other seismic source zones near plate boundaries (Rogers *et al.*, 2007). Natural variations in stratigraphy may also increase uncertainties of reference V_S soil profiles over a particular stratigraphic unit. This uncertainty can typically be reduced when subsurface geophysical and geotechnical data are available, and individual V_S soil profiles are derived from such data. Site-specific *in situ* data is always preferable when performing site-response analyses rather than using the reference profiles (Destegul, 2004; Cramer *et al.*, 2006).

For the magnitude uncertainty of NM3, we attempted to estimate its size by reproducing the ground motions. The predicted MMI of VII–VIII generated by 0.2 s SA contours during the scenario M_w 7.7 appear to be a better fit than the lower M_w 7.3 scenario event to simulate the damages reported in the wake of NM3. To further examine whether this magnitude is an appropriate estimate of NM3, we expanded the dataset to include 25 additional CEUS sites (of settlements in the late eighteenth and early nineteenth centuries) outside southeastern Missouri and researched their site conditions. We calculated 0.2 s SA and PGV as a function of the magnitudes and estimated the threshold magnitude to produce the reported MMIs during NM3. When site conditions were considered and the mode of threshold magnitudes assumed to be M_w 7.6, the best correlations with reported MMIs were achieved. The median and the mean magnitudes were found to be M_w 7.7. These results suggest that M_w 7.7 would be the most likely magnitude of NM3. The estimated magnitude is the same as that of Cramer and Boyd (2014). Our results also suggest that the magnitude of NM3 would be overestimated from M_w 7.7 to 8.1 when soil amplification effects are ignored.

Data and Resources

We obtained and analyzed data from the following sources: V_S data from D. J. Hoffman (personal comm., 2008) of the University of Science and Technology, standard penetration test profiles from C. M. Watkins (personal comm., 2011) of the U.S. Geological Survey, digital elevation models from http://data.geocomm.com (last accessed April 2013), interpolation using ArcGIS software v.9.3, Stochastic Method SIMulation from http://daveboore.com (last accessed February 2014), V_{S30} map from http://earthquake.usgs.gov/hazards/apps/vs30/ (last accessed March 2014), and Quaternary geologic maps from http://esp.cr.usgs.gov/data/quatatlas/index.shtml (last accessed April 2014).

Acknowledgments

We wish to thank David J. Hoffman (Missouri University of Science and Technology [Missouri S&T]) and Conor M. Watkins (U.S. Geological Survey, Rolla, Missouri) for supplying subsurface data. The Missouri S&T Karl F. Hasselmann Endowment funded this research. Chris Cramer (University of Memphis, Tennessee), an anonymous reviewer, and Associate Editor Mark W. Stirling significantly improved the article with their helpful comments.

References

Allen, T. I., and D. J. Wald (2009). On the use of high-resolution topographic data as a proxy for seismic site conditions (V_{S30}), *Bull. Seismol. Soc. Am.* **99,** no. 2A, 935–943.

Atkinson, G. M. (2008). Ground-motion prediction equations for eastern North America from a referenced empirical approach: Implications for epistemic uncertainty, *Bull. Seismol. Soc. Am.* **98,** no. 3, 1304–1318.

Atkinson, G. M., and I. A. Beresnev (2002). Ground motions at Memphis and St. Louis from **M** 7.5–8.0 earthquakes in the New Madrid seismic zone, *Bull. Seismol. Soc. Am.* **92,** no. 3, 1015–1024.

Atkinson, G. M., and D. M. Boore (2006). Earthquake ground-motion prediction equations for eastern North America, *Bull. Seismol. Soc. Am.* **96,** no. 6, 2181–2205.

Atkinson, G. M., and S. L. I. Kaka (2007). Relationships between felt intensity and instrumental ground motion in the central United States and California, *Bull. Seismol. Soc. Am.* **97,** no. 2, 497–510.

Bailey, J. P. (2008). Development of shear wave velocity profiles in the deep sediments of the Mississippi Embayment using surface wave and spectral ratio methods, *M.S. Thesis*, University of Missouri, Columbia, Missouri.

Bakun, W. H., and M. G. Hopper (2004). Magnitudes and locations of the 1811–1812 New Madrid, Missouri, and the 1886 Charleston, South Carolina, earthquakes, *Bull. Seismol. Soc. Am.* **94,** no. 1, 64–75.

Bakun, W. H., and C. M. Wentworth (1997). Estimating earthquake location and magnitude from seismic intensity data, *Bull. Seismol. Soc. Am.* **87,** no. 6, 1502–1521.

Bakun, W. H., A. C. Johnston, and M. G. Hopper (2002). Modified Mercalli intensities (MMI) for large earthquakes near New Madrid, Missouri, in 1811–1812 and near Charleston, South Carolina, in 1866, *U.S. Geol. Surv. Open-File Rept. 02-184*, 31 pp.

Boatwright, J., K. Thywissen, and L. Seekins (2001). Correlation of ground motion and intensity for the 17 January 1994 Northridge, California, earthquake, *Bull. Seismol. Soc. Am.* **91,** no. 4, 739–752.

Boore, D. M. (2003). Simulation of ground motion using the stochastic method, *Pure Appl. Geophys.* **160,** 635–676.

Boore, D. M. (2005). SMSIM–Fortran programs for simulating ground motions from earthquakes: Version 2.3—A revision of OFR 96-80-A, *U.S. Geol. Surv. Open-File Rept. OFR 00-509*, Denver, Colorado.

Boyd, O. (2010). Earthquake hazards (timing/recurrence/probability of an event), *Proceedings of Preparing for a Significant Central United States Earthquakes–Science Needs of the Response and Recovery Community*, *U.S. Geol. Surv. Scientific Investigations Rept. 2010-5173*, 14–20.

Building Seismic Safety Council (BSSC) (2003). *National Earthquake Hazards Reduction Program Recommended Provisions and Commentary for Seismic Regulations for New Buildings and Other Structures (FEMA 450), Part 1: Provisions*, Federal Emergency Management Agency, Washington, D.C., 356 pp.

Campbell, K. W. (2003). Prediction of strong ground motion using the hybrid empirical method and its use in the development of ground-motion (attenuation) relations in eastern North America, *Bull. Seismol. Soc. Am.* **93,** no. 3, 1012–1033.

Chapman, M. C., J. R. Martin, C. G. Olgun, and J. N. Beale (2006). Site-response models for Charleston, South Carolina, and vicinity developed from shallow geotechnical investigations, *Bull. Seismol. Soc. Am.* **96,** no. 2, 467–489.

Chung, J.-W., and J. D. Rogers (2012a). Seismic site classifications for the St. Louis urban area, *Bull. Seismol. Soc. Am.* **102,** no. 3, 980–990.

Chung, J.-W., and J. D. Rogers (2012b). Estimating the position and variability of buried bedrock surfaces in the St. Louis metro area, *Eng. Geol.* **126,** 37–45.

Collinson, C., M. L. Sargent, and J. R. Jennings (1988). Illinois basin region, in *Sedimentary Cover-North American Craton, U.S.*, L. L. Sloss (Editor), Vol. D-2, Geological Society of America, Boulder, Colorado, 383–426.

Cramer, C. H. (2001). A seismic hazard uncertainty analysis for the New Madrid seismic zone, *Eng. Geol.* **62,** nos. 1/3, 251–266.

Cramer, C. H. (2006). Quantifying the uncertainty in site amplification modeling and its effects on site-specific seismic-hazard estimation in the upper Mississippi Embayment and adjacent areas, *Bull. Seismol. Soc. Am.* **96,** no. 6, 2008–2020.

Cramer, C. H., and O. S. Boyd (2014). Why the New Madrid earthquakes are M 7–8 and the Charleston earthquake is ∼M 7, *Bull. Seismol. Soc. Am.* **104,** no. 6, 2884–2903.

Cramer, C. H., J. S. Gomberg, E. S. Schweig, B. A. Waldron, and K. Tucker (2006). First USGS urban seismic hazard maps predict the effects of soils, *Seismol. Res. Lett.* **77,** no. 1, 23–29.

Csontos, R., and R. Van Arsdale (2008). New Madrid seismic zone fault geometry, *Geosphere* **4,** no. 5, 802–813.

Dangkua, D. T., and C. H. Cramer (2011). Felt intensity versus instrumental ground motion: A difference between California and eastern North America? *Bull. Seismol. Soc. Am.* **101,** no. 4, 739–752.

Destegul, U. (2004). Sensitivity analysis of soil site response modeling in seismic microzonation for Laitput, Nepal, *M.S. Thesis*, International Institute for Geo-Information Science and Earth Observation, Enschede, The Netherlands.

Electric Power Research Institute (EPRI) (1993). *Guidelines for Determining Design Basis Ground Motions*, Electric Power Research Institute, Vol. 1, EPRI TR-102293.

Faherty, W. B. (1990). *St. Louis: A Concise History*, St. Louis Convention and Visitors Commission, St. Louis, Missouri.

Frankel, A. (2013). Comment on "Why earthquake hazard maps often fail and what to do about it" by S. Stein, R. Geller, and M. Liu, *Tectonophysics* **592,** 200–206.

Frankel, A., C. Mueller, T. Bernard, D. Perkins, E. V. Leyendecker, N. Dickman, S. Hanson, and M. Hopper (1996). National seismic-hazard maps: Documentation June 1996, *U.S. Geol. Surv. Open-File Rept. 96-532*.

Frankel, A., M. Petersen, C. Mueller, K. Haller, R. Wheeler, E. Leyendecker, R. Wesson, S. Harmsen, C. Cramer, D. Perkins, and K. Rukstales (2002). Documentation of the 2002 update of the national seismic hazard maps, *U.S. Geol. Surv. Open-File Rept. 02-420.*

Frankel, A., R. Smalley, and J. Paul (2012). Significant motions between GPS sites in the New Madrid region: Implications for seismic hazard, *Bull. Seismol. Soc. Am.* **102,** no. 2, 479–489.

Fuller, M. L. (1912). New Madrid earthquake, *U.S. Geol. Surv. Bull. 494*.

Gomberg, J., B. Waldron, E. Schweig, H. Hwang, A. Webbers, R. VanArsdale, K. Tucker, R. Williams, R. Street, P. Mayne, *et al.* (2003). Lithology and shear-wave velocity in Memphis, Tennessee, *Bull. Seismol. Soc. Am.* **93,** no. 3, 986–997.

Gray, H. H., N. K. Bleuer, J. A. Linebacker, W. C. Swadley, G. M. Richmond, R. A. Miller, R. P. Goldthwait, and R. A. Ward (1991). Quaternary Geologic Map of the Louisville 4 × 6 degrees quadrangle, United States, *U.S. Geol. Surv. Miscellaneous Investigations Series Map I–1420 (NJ-16)*, scale 1: 1,000,000, Denver, Colorado.

Haase, J. S., and R. L. Nowack (2011). Earthquake scenario ground motions for the urban area of Evansville, Indiana, *Seismol. Res. Lett.* **82,** no. 2, 177–187.

Haase, J. S., Y. S. Choi, T. Bowling, and R. L. Nowack (2011). Probabilistic seismic-hazard assessment including site effects for Evansville, Indiana, and the surrounding region, *Bull. Seismol. Soc. Am.* **101,** no. 3, 1039–1054.

Haase, J. S., C. H. Park, R. L. Nowack, and J. R. Hill (2010). Probabilistic seismic hazard estimates incorporating site effects—An example from Indiana, U.S.A, *Environ. Eng. Geosci.* **16,** no. 4, 369–388.

Hashash, Y. M. A., D. R. Groholski, C. A. Philips, D. Park, and M. Musgrove (2012). *Deepsoil: V5.1. User Manual and Tutorial*, University of Illinois, Urbana-Champaign, Illinois, 107 pp.

Hashash, Y. M. A., C. Philips, and D. Goholski (2010). Recent advances in non-linear site response analysis, *Fifth Int. Conf. on Recent Advances in Geotechnical Earthquake Engineering and Soil Dynamics*, Paper Number OSP 4, San Diego, California, 24–29 May 2010.

Hough, S. E., and S. Martin (2002). Magnitude estimates of two large aftershocks of the 16 December 1811 New Madrid earthquake, *Bull. Seismol. Soc. Am.* **92,** no. 8, 3259–3268.

Hough, S. E., and M. Page (2011). Toward a consistent model for strain accrual and release for the New Madrid seismic zone, central United States, *J. Geophys. Res.* **116,** no. 3, B03311, doi: 10.1029/2010JB007783.

Hough, S. E., J. G. Armbruster, L. Seeber, and J. F. Hough (2000). On the modified Mercalli intensities and magnitudes of the 1811–1812 New Madrid earthquakes, *J. Geophys. Res.* **105,** no. B10, 23,839–23,864.

Hough, S. E., R. Bilham, K. Mueller, W. Stephenson, R. Williams, and J. Odum (2005). Wagon loads of sand blows in White County, Illinois, *Seismol. Res. Lett.* **76,** no. 3, 373–386.

Idriss, I. M. (1990). Response of soft soil sites during earthquakes, *Proceedings of the Symposium to Honor Professor H. B. Seed*, Berkeley, California, 2 May 1990, 273–289.

Iwahashi, J., I. Kamiya, and M. Matsuoka (2010). Regression analysis of V_{S30} using topographic attributes from a 50-m DEM, *Geomorphology* **117,** nos. 1/2, 202–205.

Johnston, A. C. (1996). Seismic moment assessment of earthquakes in stable continental regions–III. New Madrid 1811–1812, Charleston 1886 and Lisbon 1755, *Geophys. J. Int.* **126,** no. 2, 314–344.

Johnston, A. C., and E. S. Schweig (1996). The enigma of the New Madrid earthquakes of 1811–1812, *Annu. Rev. Earth Planet. Sci.* **24,** 339–384.

Kaka, S. I., and G. M. Atkinson (2004). Relationships between instrumental ground-motion parameters and modified Mercalli intensity in eastern North America, *Bull. Seismol. Soc. Am.* **94,** no. 5, 1728–1736.

Karadeniz, E. (2008). Ground motion sensitivity analyses for the greater St. Louis metropolitan area, *M.S. Thesis*, Missouri University of Science & Technology, Rolla, Missouri.

Kochkin, V. G., and J. H. Crandell (2004). Survey of historical buildings predating the 1811–1812 New Madrid earthquakes and magnitude estimation based on structural fragility, *Seismol. Res. Lett.* **75,** no. 1, 22–35.

Kramer, S. L. (1996). *Geotechnical Earthquake Engineering*, Prentice Hall, Upper Saddle River, New Jersey, 653 pp.

Krinitzsky, E. L. (2002). How to obtain earthquake ground motions for engineering design, *Eng. Geol.* **65,** 1–16.

Macpherson, K. A., E. W. Woolery, Z. Wang, and P. Liu (2010). Three-dimensional long-period ground-motion simulations in the upper Mississippi Embayment, *Seimol. Res. Lett.* **81,** no. 2, 391–405.

Middendorf, M. A. (2003). Geologic Map of Missouri (Sesquicentennial Edition), Missouri Department of Natural Resources, Divisions of Geology and Land Survey.

Missouri Department of Natural Resources Division of Geology and Land Survey (MODGLS) (2007). *Missouri Environmental Geology Atlas-2007*, Missouri Department of Natural Resources Division of Geology and Land Survey, Rolla, Missouri, CD-ROM.

Missouri Department of Natural Resources Division of Geology and Land Survey (MODGLS) (2014). *The New Madrid Seismic Zone*, Missouri Department of Natural Resources Division of Geology and Land Survey, Fact Sheet, 26.

Mueller, K., and J. Pujol (2001). Three-dimensional geometry of the Reelfoot blind thrust: Implications for moment release and earthquake magnitude in the New Madrid seismic zone, *Bull. Seismol. Soc. Am.* **91,** no. 6, 1563–1573.

Mueller, K., S. E. Hough, and R. Bilham (2004). Analyzing the 1811–1812 New Madrid earthquakes with recent instrumentally recorded aftershocks, *Nature* **429,** 284–288.

Newman, A., J. Schneider, S. Stein, and A. Mendez (2001). Uncertainties in seismic hazard maps for the New Madrid seismic zone and implications for seismic hazard communication, *Seismol. Res. Lett.* **72,** no. 6, 647–663.

Odum, J. K., W. J. Stephenson, K. M. Shedlock, and T. L. Pratt (1998). Near-surface structural model for deformation associated with the February 7, 1812, New Madrid, Missouri, earthquake, *Bull. Geol. Soc. Am.* **110,** no. 2, 149–162.

Ohta, Y., and N. Goto (1978). Empirical shear wave velocity equations in terms of characteristic soil indexes, *Earthq. Eng. Struct. Dynam.* **6,** no. 2, 167–187.

Petersen, M. D., A. D. Frankel, S. C. Harmsen, C. S. Mueller, K. M. Haller, R. L. Wheeler, R. L. Wesson, Y. Zeng, O. S. Boyd, D. M. Perkins, *et al.* (2008). Documentation for the 2008 update of the United States national seismic hazard maps, *U.S. Geol. Surv. Open-File Rept. 2008-1128*, 61 pp.

Petersen, M. D., M. P. Moschetti, P. M. Powers, C. S. Mueller, K. M. Haller, A. D. Frankel, Y. Zeng, S. Rezaeian, S. C. Harmsen, O. S. Boyd, *et al.* (2014). Documentation for the 2014 update of the United States national seismic hazard maps, *U.S. Geol. Surv. Open-File Rept. 2014-1091*, 243 pp.

Pezeshk, S., A. Zandieh, and B. Tavakoli (2011). Hybrid empirical ground-motion prediction equations for eastern North America using NGA models and updated seismological parameters, *Bull. Seismol. Soc. Am.* **101,** no. 4, 1859–1870.

Ramírez-Guzmán, L., O. S. Boyd, S. Hartzell, and R. A. Williams (2012). Seismic velocity model of the central United States (version 1): Description and simulation of the 18 April 2008 Mt. Carmel, Illinois, earthquake, *Bull. Seismol. Soc. Am.* **102,** no. 6, 2622–2645.

Rogers, J. D., D. Karadeniz, and C. K. Kaibel (2007). Seismic response modeling for Missouri River highway bridges, *J. Earthq. Eng.* **11,** no. 3, 400–424.

Romero, S., and G. J. Rix (2001). Regional variations in near surface shear wave velocity in the greater Memphis area, *Eng. Geol.* **62,** nos. 1/3, 137–158.

Romero, S., and G. J. Rix (2005). Ground motion amplification of soils in the upper Mississippi Embayment, Mid-America Earthquake Center, University of Illinois at Urbana-Champaign, Illinois, 461 pp, Report No. GIT-CEE/GEO-01-1.

Santi, P. M., E. J. Neuner, and N. L. Anderson (2002). Preliminary evaluation of seismic hazards for emergency rescue route, U.S. 60, Missouri, *Environ. Eng. Geosci.* **8,** no. 4, 261–277.

Seed, H. B., and J. I. Sun (1987). Relationship between soil conditions and earthquake ground motions in Mexico City in the earthquake of Sept. 19, 1985, *Earthq. Spectra* **4,** no. 4, 687–730.

Seed, H. B., M. P. Romo, J. I. Sun, A. Jaime, and J. Lysmer (1988). The Mexico earthquake of September 19, 1985: Relationships between soil conditions and earthquake ground motions, *Earthq. Spectra* **4,** 687–729.

Seed, H. B., C. Ugas, and J. Lysmer (1976). Site-dependent spectra for earthquake-resistant design, *Bull. Seismol. Soc. Am.* **66,** no. 1, 221–243.

Silva, W., N. Gregor, and R. Darragh (2002). Development of regional hard rock attenuation relations for central and eastern North America, *Technical Report*, Pacific Engineering and Analysis, El Cerrito, California, 57 pp.

Somerville, P., N. Collins, N. Abrahamson, R. Graves, and C. Saikia (2001). Ground motion attenuation relations for the central and eastern United States, *Final Report to U.S. Geol. Surv.*, 38 pp.

St. Louis City Planning Commission (1969). *History: Physical Growth of the City of St. Louis*, St. Louis City Planning Commission, St. Louis, Missouri.

Street, R., D. Hoffman, and J. Kiefer (2004). Comment on "Survey of historical buildings predating the 1811–1812 New Madrid earthquakes and magnitude estimation based on structural fragility" by Vladimir G. Kochkin and Jay H. Crandell, *Seismol. Res. Lett.* **75,** no. 6, 744–746.

Tavakoli, B., and S. Pezeshk (2005). Empirical-stochastic ground-motion prediction for North America, *Bull. Seismol. Soc. Am.* **95,** no. 6, 2283–2296.

Toro, G. R., and W. J. Silva (2001). Scenario earthquakes for Saint Louis, MO, and Memphis, TN, and seismic hazard maps for the central United States region including the effect of site conditions, *Final Technical Report to the U.S. Geol. Surv.*, Risk Engineering, Inc., Boulder, Colorado.

Toro, G. R., N. A. Abrahamson, and J. F. Schneider (1997). Model of strong ground motions from earthquakes in central and eastern North America: Best estimates and uncertainties, *Seismol. Res. Lett.* **68,** no. 1, 41–57.

Tuttle, M. P., E. S. Schweig, J. D. Sims, R. H. Lafferty, L. W. Wolf, and M. L. Haynes (2002). The earthquake potential of the New Madrid seismic zone, *Bull. Seismol. Soc. Am.* **92,** no. 6, 2080–2089.

Van Arsdale, R. B., D. Pryne, and W. Edward (2013). Northwestern extension of the Reelfoot north fault near New Madrid, Missouri, *Seismol. Res. Lett.* 84**,** no. 6, 1114–1123.

Van Arsdale, R. B., R. A. Williams, E. S. Schweig, K. M. Shedlock, J. K. Odum, and K. W. King (1995). The origin of Crowley's Ridge, northeastern Arkansas: Erosional remnant or tectonic uplift? *Bull. Seismol. Soc. Am.* **85,** no. 4, 963–986.

Wald, D. J., and T. I. Allen (2007). Topographic slope as a proxy for seismic site conditions and amplification, *Bull. Seismol. Soc. Am.* **97,** no. 5, 1379–1395.

Wald, D. J., V. Quitoriano, T. Heaton, and H. Kanamori (1999). Relationships between peak ground acceleration, peak ground velocity, and modified Mercalli intensity in California, *Earthq. Spectra* **15,** 557–564.

Whitfield, J. W. (1982). Surficial materials map of Missouri, *Missouri Geological Survey*, Rolla, Missouri.

Whitfield, J. W., R. A. Ward, J. E. Denne, D. F. Holbrook, W. V. Bush, J. A. Lineback, K. V. Luza, K. M. Jensen, W. D. Fishman, G. M. Richmond, and D. L. Wiede (1993). Quaternary Geologic Map of the Ozark Plateau 4 × 6 degrees quadrangle, United States, *U.S. Geol. Surv. Miscellaneous Investigations Series Map I–1420 (NJ-15)*, Denver, Colorado, scale 1: 1,000,000.

Williams, R. A., R. L. Dart, and C. M. Volpi (2010). Bicentennial of the 1811–1812 New Madrid earthquake sequence December 2011–2012, *U.S. Geol. Surv. General Information Product 118*, Denver, Colorado.

Appendix

To calculate 0.2 s spectral acceleration and peak ground velocity, we employed the regression equation derived by

Table A1
Geologic Units in the Study Area

Era	Period	Geologic Unit	Material
Cenozoic	Quaternary	Alluvium	Clay, silt, sand, and gravel
	Tertiary	Claiborne	Sand, silt, and clay
		Wilcox sandstone	Sandstone, clay, and gravel
		Midway group	Clay and sand
Mesozoic	Cretaceous	McNairy formation	Sandstone with clay and gravel
Paleozoic	Ordovician	Powell dolomite	Silty cherty dolomite and chert with sandstone beds
		Jefferson City dolomite	
		Roubidoux formation	Sandstone, chert, and dolomite
		Gasconade dolomite	Cherty dolomite
	Cambrian	Eminence dolomite	Dolomite with chert

Modified from Middendorf (2003).

Atkinson and Boore (2006) for the central and eastern United States:

$$\log \mathrm{PSA} = c_1 + c_2 M + c_3 M^2 + (c_4 + c_5 M) f_1 + (c_6 + c_7 M) f_2 + (c_8 + c_9 M) f_0 + c_{10} R_{\mathrm{cd}} + S, \quad \text{(A1)}$$

in which PSA is pseudospectral acceleration with 5% damping; M is moment magnitude; R_{cd} is distance to the fault (km); $f_0 = \max(\log(10/R_{\mathrm{cd}}), 0)$; $f_1 = \min(\log R_{\mathrm{cd}}, \log 70)$; $f_2 = \max(\log(R_{\mathrm{cd}}/140), 0)$; and S is the soil amplification factor (e.g., hard-rock sites = 0). Refer to Atkinson and Boore (2006) equation (5) and table 6 for c coefficients, and equations (7a–8d) and tables (8–9) for soil amplification factors. The geologic units are described in Table A1. The generalized geologic cross section (west to east) of the upper Mississippi Embayment is shown in Figure 2.

Missouri University of Science and Technology
Department of Geosciences and Geological and Petroleum Engineering
1400 N Bishop Avenue
Rolla, Missouri 65409
jc8r4@mst.edu
rogersda@mst.edu

Manuscript received 13 October 2014;
Published Online 26 May 2015